

# The Effect of the Rolling Mode on the Recrystallization Behavior of 2090 Al-Li Alloy

O.S. Es-Said, F. Fisher, D. Johansen, J. Quattrocchi, D. Raizk, C. Ventura, K. Zakharia, D. Ruhl, N. Khankan, M. Rajabi, R. Archilla, and H. Petel

As-received 2090 Al-Li hot-rolled plate was homogenized at 482 °C for 10 h and cold worked to 95% reduction in thickness. The rolling modes were varied. One group of samples was rolled longitudinally parallel to the hot-rolling direction, the second transversely to the rolling direction, the third at 45° to the rolling direction, and the fourth in all three modes. All four groups were subsequently annealed at 456 °C for 24 h. The effect of varying the rolling mode on the ductility and strength was studied by examining the kinetics of softening as a function of the annealing time. All the groups recrystallized in less than 1 h with a coarse, elongated grain structure. Although the strengths of the different groups were similar, the ductilities varied significantly.

## Keywords

aluminum alloy 2090, anisotropy, recrystallization, rolling

## 1. Introduction

IN recent years Al-Li alloys have received considerable attention from both scientific and industrial communities because of their high modulus/density property, which is especially attractive for aerospace applications. However, their poor ductility limits the number of service applications. The poor ductility has been attributed to the intense coplanar slip during deformation associated with the shearable  $\delta'$  ( $\text{Al}_3\text{Li}$ ) precipitates and the soft precipitate-free zones (PFZ) resulting from the heterogeneous precipitation of  $\delta$  ( $\text{AlLi}$ ) precipitates along grain boundaries (Ref 1, 2). The PFZs act as an intergranular propagation medium for cracks initiating at grain-boundary precipitates or triple junctions (Ref 2). Microstructural control through thermomechanical processing and modifications in alloy chemistry might be expected to improve the poor ductility in Al-Li alloys. Generally, ductility is improved after recrystallization at the expense of mechanical strength. Accordingly, the present study investigates the effect of varying the rolling mode on the ductility and strength of a 2090 Al-Li alloy after recrystallization.

## 2. Experimental Method

The 2090 Al-Li alloy provided by Kaiser Aluminum has a composition of 2.08 wt% Li, 2.89 wt% Cu, 0.12 wt% Zr, and 0.06 wt% Si. The material was direct-chill cast into a 406 mm thick ingot, scalped to 381 mm, and then hot rolled to 38.1 mm plates. The starting hot-rolling temperature was 482 to 496 °C and the exit temperature was 371 °C. Each reduction pass (cross-rolling) reduced the material 38.1 mm. The plates were then solution treated at 543 °C for 2 h, stretched 7%, and aged

at room temperature. The as-received plate was  $406.4 \times 406.4 \times 38.1$  mm.

The fabricating schedule given in Fig. 1 was designed to study the effect of the rolling mode on the recrystallization behavior of the 2090 Al-Li alloy. The material was cut into 9.5 mm thick samples, homogenized at 482 °C for 10 h, and then cold rolled to 95% reduction in thickness in four directions. The first was along the longitudinal direction of the initial hot rolling, the second was along the transverse direction (long transverse), the third along a 45° angle to the rolling direction, and the last along the 45°, longitudinal, and transverse directions in equal increments. The straight rolling mode is shown in Fig. 2.

The rolled samples with a thickness of 0.51 mm were then annealed at 454 °C up to 24 h. Softening after 1, 10, and 24 h was studied using Rockwell superficial (15 T) measurements and metallographic procedures. Electrical resistivity measurements were used to monitor the changes in solute solid concentration of the alloy. The stress-strain characteristics were determined at room temperature at a constant crosshead speed (1.27 mm/min) by using a screw-driven Instron machine (Model 4505) in a uniaxial tension mode. All the samples were

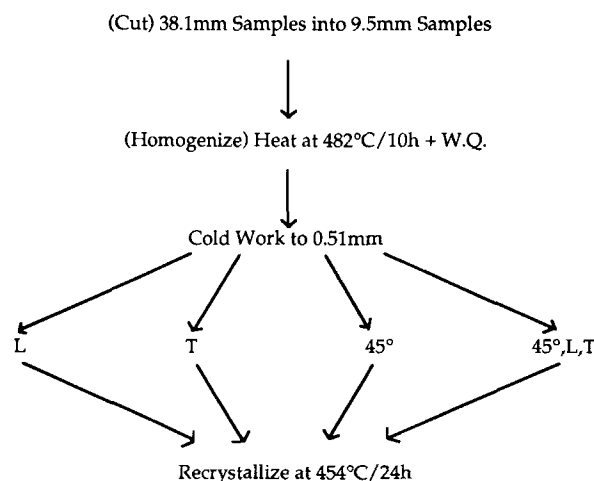


Fig. 1 Thermomechanical procedure. W.Q., water quench; L, longitudinal; T, transverse

O.S. Es-Said, F. Fisher, D. Johansen, J. Quattrocchi, D. Raizk, C. Ventura, K. Zakharia, D. Ruhl, N. Khankan, M. Rajabi, R. Archilla, and H. Petel, Mechanical Engineering Department, Loyola Marymount University, Los Angeles, CA 90045, USA

machined with a Tensilkut router from the as-rolled sheet with the tensile axis parallel to the rolling direction. Three specimens were prepared for each test condition, with each data point representing the mean of three tests.

### 3. Results

The microstructure of the as-received hot-rolled plate is shown in Fig. 3. The grains in the longitudinal section are several millimeters in length and vary in width from 20 to 100  $\mu\text{m}$ . In the transverse section the grain size is approximately 300  $\mu\text{m}$  in length. After the homogenization treatment at 482  $^{\circ}\text{C}$  for 10 h, the grain structure was virtually unaltered, due to the  $\beta'$  ( $\text{Al}_3\text{Zr}$ ) particle effect (Ref 1) (Fig. 4).

The deformation of all the samples rolled in the four modes showed similar patterns. The longitudinal view revealed a

wavy pattern with triple points and grain-boundary intersections. This, together with the presence of large intermetallic particles, can provide nucleation sites for the newly recrystallized grains. The transverse view, on the other hand, revealed parallel microbands with a less intense deformation. It would be expected that the rate of nucleation of recrystallization would be greater in the heavily deformed wavy region. The deformation pattern for samples rolled in the transverse direction is shown in Fig. 5.

Figures 6 and 7 show superficial hardness and mechanical data for the samples that were rolled to 95% reduction in thickness in the four different modes and isothermally annealed at 454  $^{\circ}\text{C}$  for 24 h. The reduction in superficial hardness (15 T) and mechanical stresses for all the samples indicated that full recrystallization was achieved in less than 1 h. Microscopic observations indicated that full recrystallization was achieved in less than 30 min (Table 1).

The microstructures of all the samples revealed full recrystallization. The recrystallized grains were elongated. The grain sizes were finer in the longitudinal view, which accords with the earlier observation that the rate of nucleation of recrystallized grains would be expected to be high in the wavy heavily deformed region. The grain structure was inhomogeneous with a relatively large grain size distribution. The grain sizes are summarized in Table 1. The width of all the recrystallized grains was about 25 to 50  $\mu\text{m}$ . We will define the ratio of the length of the recrystallized grains in the transverse view to that in the longitudinal view as  $R$ . The  $R$  value is 2.5 for samples rolled in the longitudinal direction, 3 for samples rolled in the transverse direction, 2 for samples rolled in the 45 $^{\circ}$  direction, and 1.5 for samples rolled in all three modes (Fig. 8). As the 45 $^{\circ}$  rolling is employed, the difference in the length of the recrystallized grain sizes along the longitudinal and transverse views becomes less pronounced (Table 1).

### 4. Discussion

In the 2090 alloy system, lithium is added to reduce the density and maximize the elastic modulus. During aging, lithium

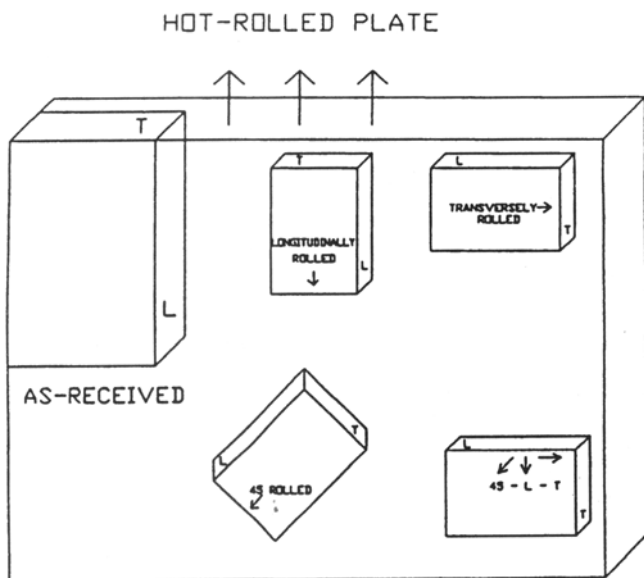


Fig. 2 Rolling modes

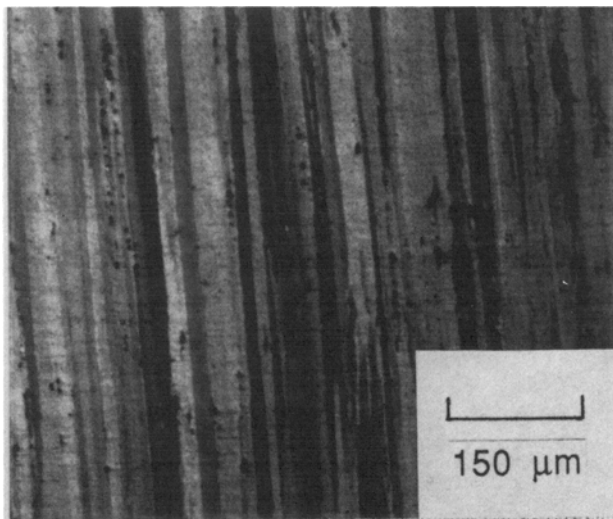
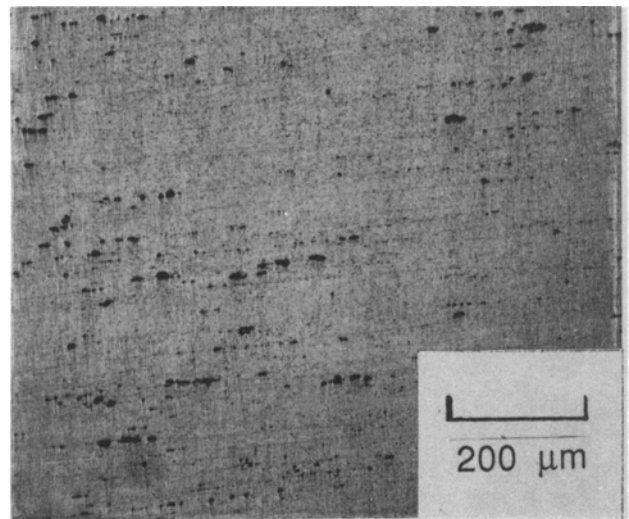


Fig. 3 Grain and particle structure of 2090 Al-Li alloy as-received (longitudinal view)



together with copper forms strengthening precipitates, mainly  $\delta'$  ( $\text{Al}_3\text{Li}$ ),  $T_1$  ( $\text{Al}_2\text{CuLi}$ ), and  $\theta'$  ( $\text{Al}_2\text{Cu}$ ), together with equilibrium precipitates  $T_2$  ( $\text{Al}_6\text{CuLi}_3$ ) and  $\delta$  ( $\text{AlLi}$ ) (Ref 1) Zirconium forms coherent precipitates of  $\beta'$  ( $\text{Al}_3\text{Zr}$ ), and although these have a limited strengthening effect (Ref 3), they are effective pinning sites preventing grain and subgrain migration during solutionization (Ref 1) and in dynamic and static recrystallization (Ref 4).

The constitutional variables that might retard recrystallization in this alloy system are the segregation of solute atoms, especially lithium, and the effect of the zirconium-bearing particles. At high concentrations of solute atoms (supersaturation), the subgrain boundaries will be held by the solute atoms (solute segregation) (Ref 5). However, with prolonged anneal-

ing at an elevated temperature, full recrystallization is achieved (Ref 6). It appears from a recent study by the present authors (Ref 6) that the loss of supersaturation content is the controlling factor in obtaining full recrystallization in the alloy system under consideration.

The electrical resistivity changes of all the samples rolled in the four different modes are shown in Fig. 9. The electrical resistivity changes show a drop of about 30% in all the samples rolled and aged for 24 h, suggesting that solute segregation was significantly reduced. It is well established that all solute additions to aluminum raise its electrical resistivity (Ref 7-9). If the solute precipitates out of solid solution, the electrical resistivity decreases because a precipitate is not an effective electron scatterer, as is the solute in solution. The effects of the solutes pre-

**Table 1 Grain sizes (linear intercepts) of the recrystallized structures**

Mode of rolling	Isothermal anneal at 454 °C for:				
	0.5 h	1 h	5 h	10 h	24 h
<b>Longitudinal direction</b>					
Longitudinal view					100-175 $\mu\text{m}$ in length, 30-40 $\mu\text{m}$ in width
Transverse view			300-400 $\mu\text{m}$ in length, 25-30 $\mu\text{m}$ in width	300-400 $\mu\text{m}$ in length, 25-30 $\mu\text{m}$ in width	300-400 $\mu\text{m}$ in length, 30-40 $\mu\text{m}$ in width
<b>Transverse direction</b>					
Longitudinal view		125-175 $\mu\text{m}$ in length, 20-40 $\mu\text{m}$ in width			
Transverse view	400-500 $\mu\text{m}$ in length, 30-40 $\mu\text{m}$ in width				400-500 $\mu\text{m}$ in length, 30-40 $\mu\text{m}$ in width
<b>45° direction</b>					
Longitudinal view		100-200 $\mu\text{m}$ in length, 30-40 $\mu\text{m}$ in width		100-200 $\mu\text{m}$ in length, 30-40 $\mu\text{m}$ in width	
Transverse view	150-300 $\mu\text{m}$ in length, 20-40 $\mu\text{m}$ in width		200-400 $\mu\text{m}$ in length, 20-30 $\mu\text{m}$ in width	250-400 $\mu\text{m}$ in length, 30-30 $\mu\text{m}$ in width	300-400 $\mu\text{m}$ in length, 40-50 $\mu\text{m}$ in width
<b>45° L-T direction</b>					
Longitudinal view		100-200 $\mu\text{m}$ in length, 20-30 $\mu\text{m}$ in width		100-200 $\mu\text{m}$ in length, 30-40 $\mu\text{m}$ in width	100-250 $\mu\text{m}$ in length, 30-40 $\mu\text{m}$ in width
Transverse view		150-200 $\mu\text{m}$ in length, 20-30 $\mu\text{m}$ in width		150-300 $\mu\text{m}$ in length, 30-40 $\mu\text{m}$ in width	

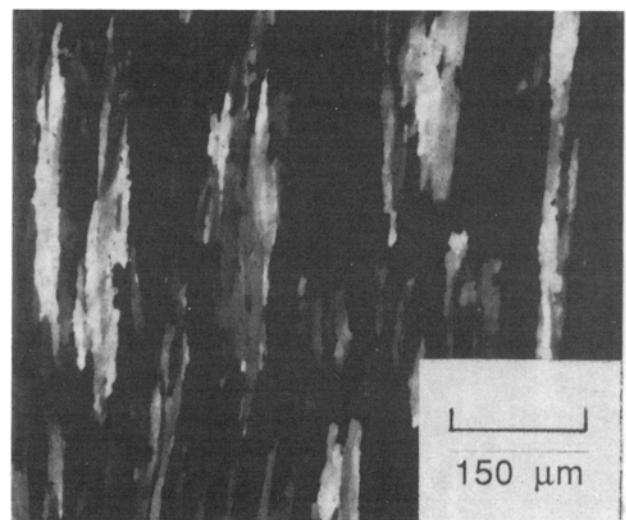
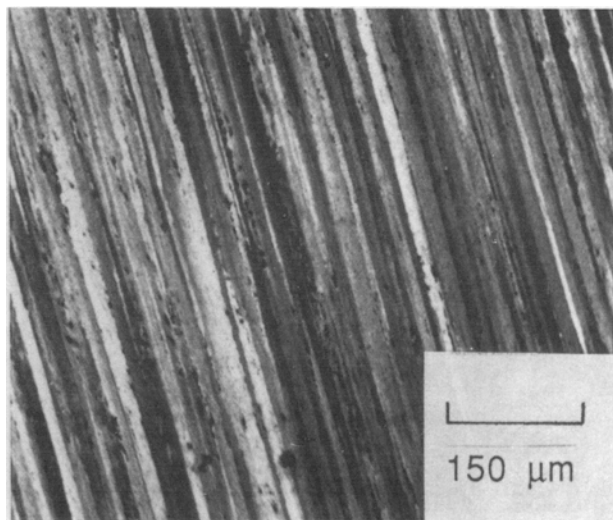


**Fig. 4** Grain structure of 2090 Al-Li alloy homogenized at 454 °C/10 h (longitudinal and transverse views)

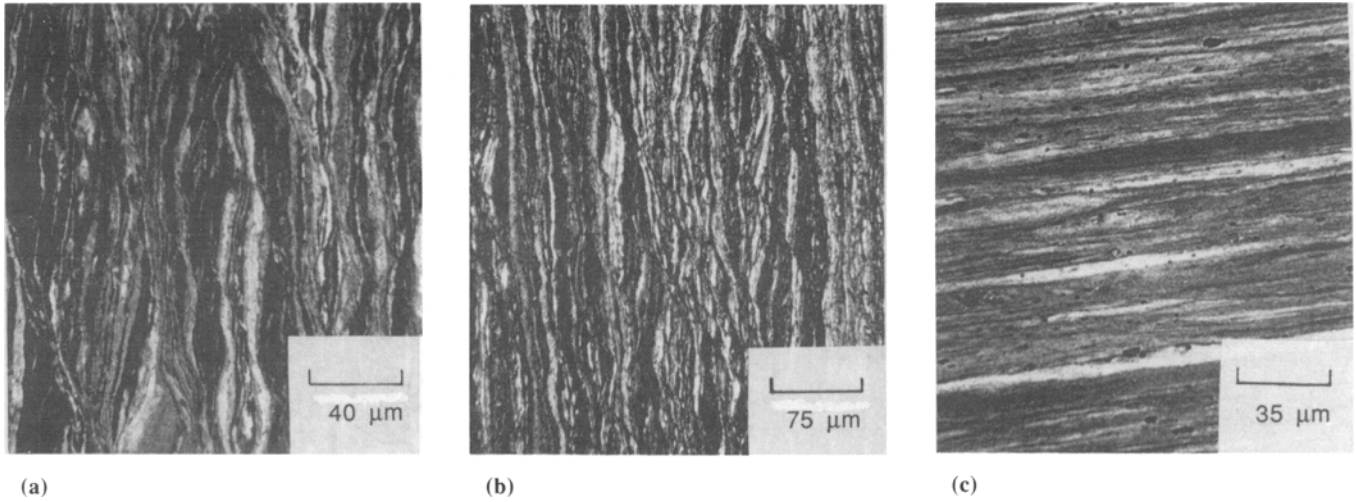


**Fig. 5** Grain structures of 2090 Al-Li alloy homogenized and rolled to 0.51 mm in the transverse direction. (a) and (b) Longitudinal views. (c) Transverse view

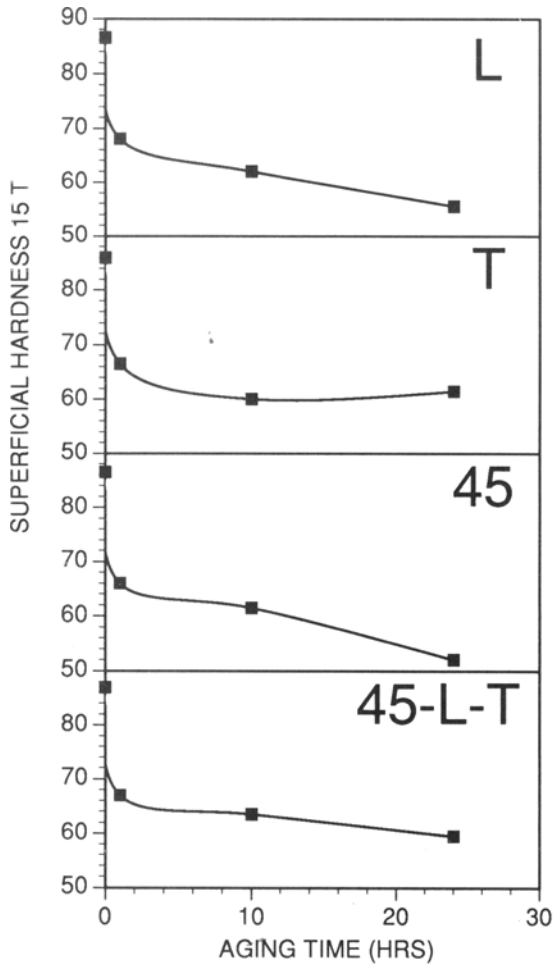


**Fig. 6** Superficial hardness changes at 454 °C for 24 h. L, longitudinal; T, transverse

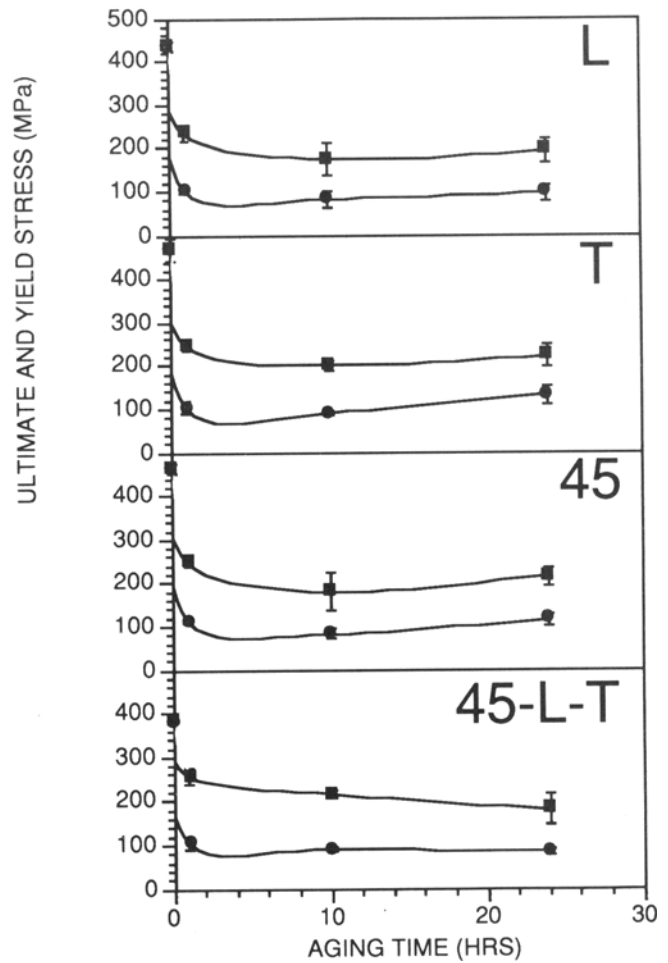


**Fig. 7** Ultimate (and yield) stress changes at 454 °C for 24 h. L, longitudinal; T, transverse

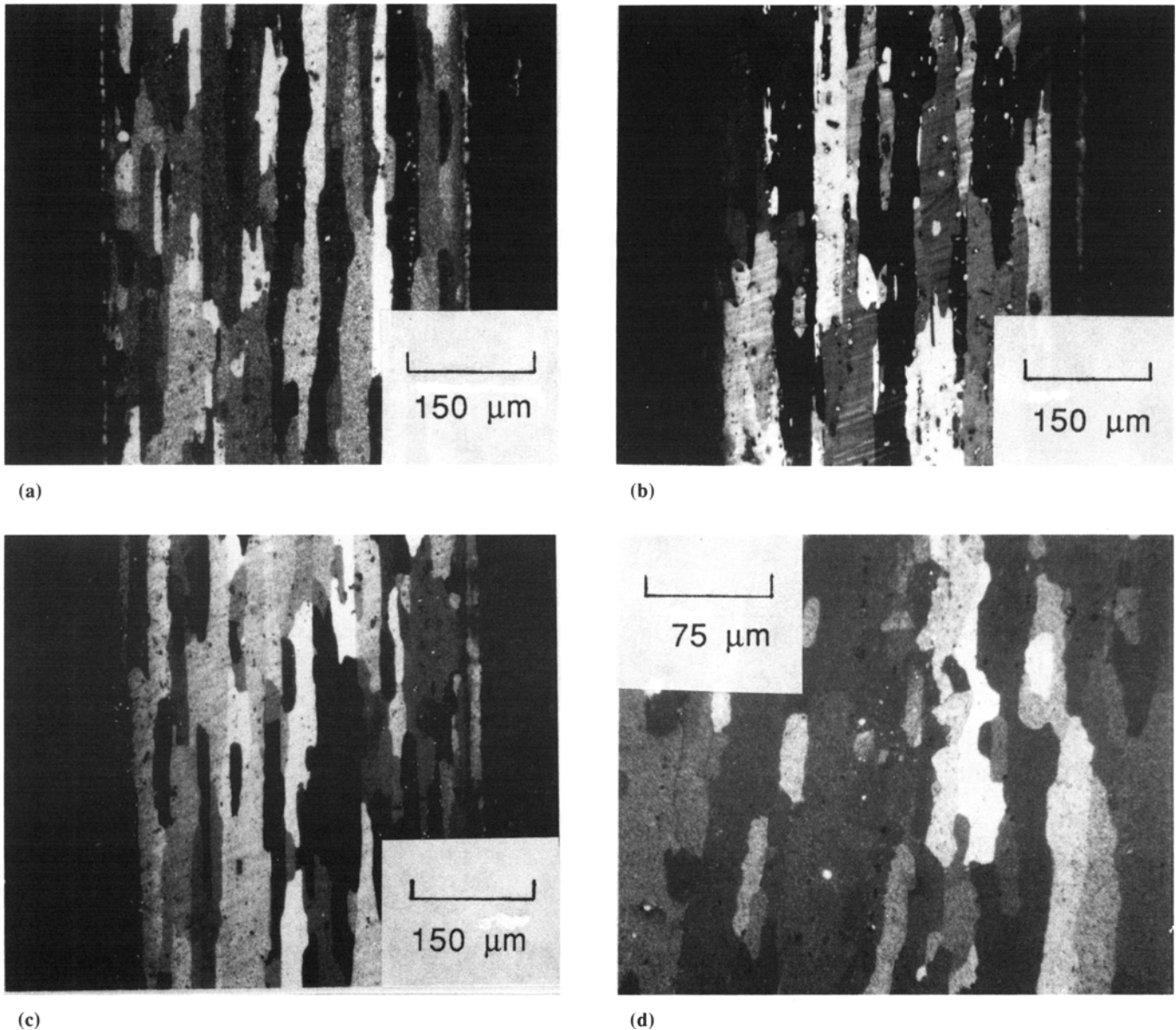


**Fig. 8** Grain structure of 2090 Al-Li alloy, homogenized and cold worked to 0.51 mm in the longitudinal direction (a), transverse direction (b), 45° direction (c), and 45°-L-T direction (d). (Transverse views.)

sent in the 2090 Al-Li alloy (lithium, copper, silicon, and zirconium) on raising the electrical resistivity of aluminum when they are *in solution* are 3.31, 0.344, 1.02, and 1.74  $\mu\Omega \cdot \text{cm}$  (per wt%), respectively (Ref 8). Their effects when they are *out of solution* are 0.68, 0.03, 0.088, and 0.044  $\mu\Omega \cdot \text{cm}$  (per wt%), respectively. Their effects when in solid solution are 4.9, 11.5, 11.6, and 39.5 times what they are when they are out of solution. Hence the onset of recrystallization in all samples might be explained in terms of the loss of solute segregation effects.

The shape of the elongated grains has been explained by different mechanisms. Makin and Stobbs (Ref 10) attribute it to a subgrain coalescence mechanism in an Al-Li-Zr alloy. They indicate that an alloy in the deformed state forms bands of elongated and misoriented cells, which consequently form subgrains that develop into elongated grains in the rolling direction. However, in this study, elongated grains also devel-

oped in transverse directions to all the rolling modes and were more pronounced. Goncalves and Sellars (Ref 11) attribute the formation of elongated grains in other Al-Li systems to the pinning effect of an inhomogeneous and elongated distribution of lithium dispersion. Es-Said et al. (Ref 12) relate the formation of elongated grains in an Al-Mn system to particle-affected nucleation of recrystallization. Noble et al. (Ref 13) and Palmer et al. (Ref 14) relate the formation of elongated grains to the addition of zirconium, where the equiaxed grains of Al-Li alloys transform to elongated grains by the modification of the microstructure. The complex deformation pattern with its associated texture data more likely would explain the preferential growth of recrystallized grains.

Anisotropy in strength and ductility in the Al-Li sheet material has been reported by several authors. Palmer et al. (Ref 14) observed pronounced anisotropy in strength and ductility in a

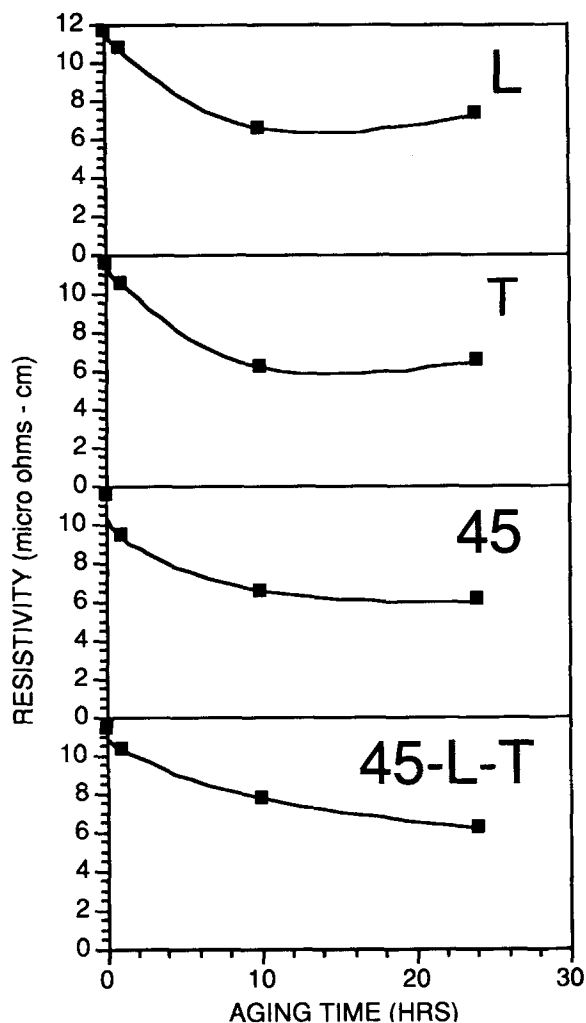


Fig. 9 Electrical resistivity changes at 454 °C for 24 h. L, longitudinal; T, transverse

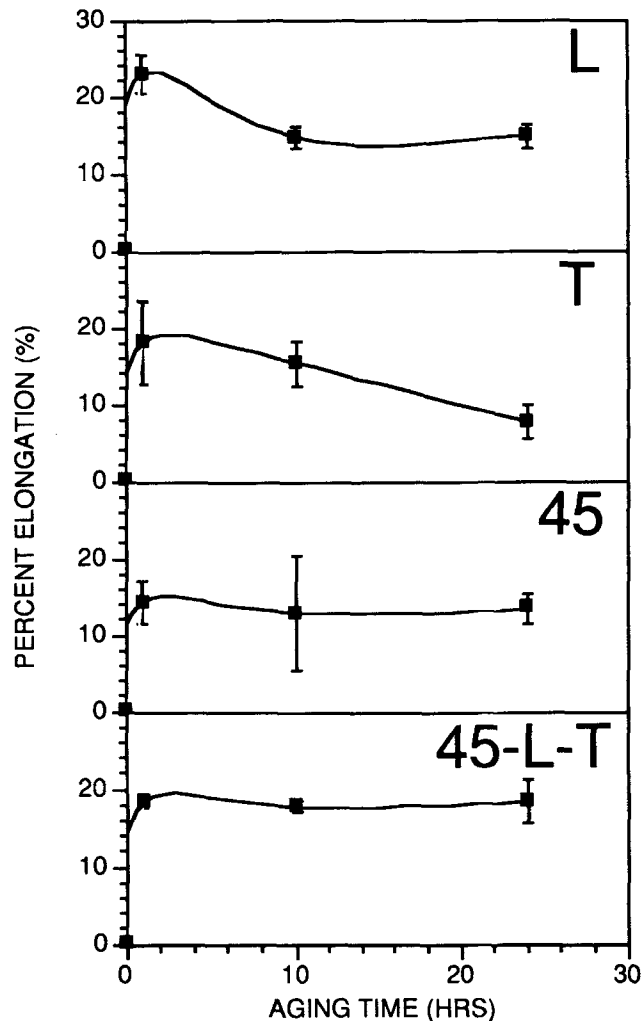


Fig. 10 Percent elongation changes at 454 °C for 24 h. L, longitudinal; T, transverse

conventionally processed Al-Li-Cu-Mg-Zr unrecrystallized sheet where the anisotropy was significantly reduced after recrystallization. They indicate that differences in behavior between longitudinal and transverse sections in the unrecrystallized state are dependent on the strain path, where intermetallics are aligned in the principal strain direction together with a crystallographic texture such that active slip systems produce a strong shearing component across the intermetallic particles in the transverse direction. Cho et al. (Ref 15) researched samples fabricated from a superplastically formable high-strength 2090 sheet that was rolled in the longitudinal (L), transverse (T), and 45° orientations with respect to the original rolled direction. They report that the strength in the L-direction was slightly higher than the other directions, and that the strength levels in the T-direction and the 45°-direction were identical, with a maximum in ductility in the L-direction and a minimum in the T-direction. These results are not in accord with those typically observed for conventional 2090 sheet, where the 45°-direction yield strength is typically much lower than that in the L- or T-directions, and accordingly more ductile.

In the present study, the initial strength levels (cold-worked condition) of the L, T, and 45° samples were similar, while strength of the 45°-L-T samples was slightly lower. However, the rates of drop in strength with the onset of recrystallization were almost identical (Fig. 7).

The ductility results show some anisotropy (Fig. 10). The best results were obtained in the 45°-L-T condition, where the percent elongation rose to 18% compared to the cold-worked state and maintained that level.

The low ductility of Al-Li alloys is attributed to slip localization through the  $\delta'$  ( $\text{Al}_3\text{Li}$ ) phase. Deformation proceeds by dislocations shearing the  $\delta'$  precipitates, and their reduction in cross-sectional area encourages planar inhomogeneous slip, leading to loss of ductility (Ref 3). Hence although  $\delta'$  is the primary strengthening phase, it also embrittles the alloy through concentrating the deformation in intense slip bands, resulting in premature failure. It appears that the onset of the 45° rolling mode or preferably the combined rolling mode (45°-L-T) had the effect of diffusing the localized slip bands and hence increasing the homogeneity of plastic flow.

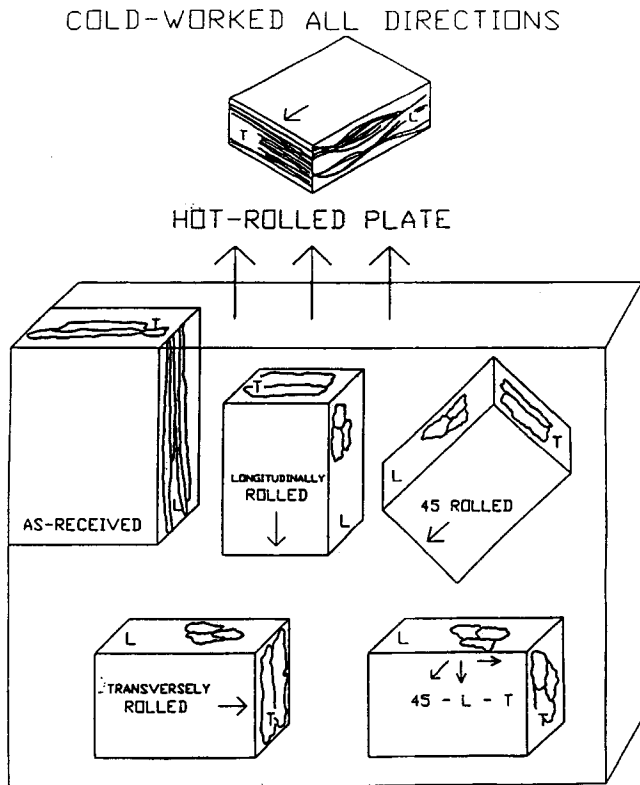


**Fig. 11** Microstructural summary

The reduction in elongation with aging in the L- and T-conditions cannot be explained by a change in composition, the presence of oxide particles (Ref 16), or appreciable grain growth (Ref 8). A possible explanation is grain-boundary precipitation (Ref 17) associated with the coarse, elongated grains in the L- and T-directions, together with the inhomogeneity of the grain sizes in the L-view and T-view of each rolling mode, *the R value previously defined*. The *R* values were 2.5 in the L-condition and 3 in the T-condition as compared to 2 and 1.5 in the 45° and 45°-L-T conditions, and it is well established that coarse elongated grains are associated with low ductility (Ref 18). The microstructural results are schematically illustrated in Fig. 11 to summarize our findings in terms of the inhomogeneity of the grain sizes in the transverse and longitudinal views of the four rolling modes.

## 5. Conclusions

- All the samples rolled in the four different modes recrystallized at 454 °C. The grain structure was inhomogeneous; the grains were coarse and elongated.
- The recrystallized grains in the transverse view of all modes of rolling were longer than in the longitudinal view. The *R* ratio (the ratio of the length of the recrystallized grains in the transverse view to that in the longitudinal view) was 2.5 for samples rolled in the L-direction, 3 in the T-direction, 2 in the 45° direction, and 1.5 in the 45°-L-T direction.

- The strengths in all the recrystallized conditions were similar independent of the rolling direction; however, the ductility behavior was dependent on the rolling direction. The ductility improved with the onset of 45° rolling and was best with a combined rolling mode (45°-L-T).

## Acknowledgements

The authors are grateful to Kaiser Aluminum at Pleasanton, CA for providing the material. The authors wish to thank Dr. J.P. Callinan, Mrs. O. Rivera, and Mr. Ray Stits for their help in preparing the manuscript.

## References

1. F.S. Lin, S.B. Chakraborty, and E.A. Starke, Jr., Microstructure-Property Relationships of Two Al-3Li-2Cu-0.2Zr-XCd Alloys, *Metall. Trans. A*, Vol 13, March 1982, p 401-410
2. E.A. Starke, Jr. and F.S. Lin, The Influence of Grain Structure on the Ductility of the Al-Cu-Li-Mn-Cd Alloy 2020, *Metall. Trans. A*, Vol 13, Dec 1982, p 2259-2269
3. W. Wang and M. Wells, Microstructure and Mechanical Behavior of Al-Li-Zr Alloys, *Proceedings of Light-Weight Alloys for Aerospace Applications II*, TMS, 1991, p 189-202
4. L.S. Collier, K. Ranganathan, and T.H. Sanders, Jr., Recrystallization Resistance in Al-Li Alloys Containing Zirconium, *Proceedings of Light-Weight Alloys for Aerospace Applications II*, TMS, 1991, p 141-155
5. K. Lucke and H.P. Stuwe, On the Theory of Impurity Controlled Grain Boundary Migration, *Acta Met.*, Vol 19, 1971, p 1087-1099
6. J. Quattrocchi, D. Johansen, M. O'Brien, N. Khankan, C. Ventura, D. Raizk, K. Zakharia, M. Rajabi, R. Archilla, D. Ruhl, H. Petel, K. Shin, C. Louie, F. Fisher, and O.S. Es-Said, On the Transformation Characteristics of 2090 Al-Li Alloy, *Proceedings of Light-Weight Alloys for Aerospace Applications II*, TMS, 1991, p 107-140
7. F.R. Fickett, A Review of Resistive Mechanisms in Aluminum, *Cryogenics*, Oct 1971, p 349-367
8. W.A. Dean, Effects of Alloying Elements and Impurities on Properties, in *Aluminum: Properties, Physical Metallurgy and Phase Diagrams*, Vol 1, American Society for Metals, 1967, p 174-176
9. O.S. Es-Said and J.G. Morris, A Method to Calculate the Resistivity of Strip Cast 3000 Series Al Alloys Based on Their Nominal Solute Content, *Proceedings of Nondestructive Characterization of Materials II*, Plenum Press, 1986, p 271-279
10. P.L. Makin and W.M. Stobbs, Comparison of Recrystallization Behavior of an Al-Li-Zr Alloy with Related Binary Systems, *Proceedings of Aluminum Lithium Alloys III*, Institute of Metals, 1985, p 392-401
11. M. Goncalves and C.M. Sellars, Static Recrystallization after Hot Working of Al-Li Alloys, *J. Phys.*, Vol 48 (No. C3), Suppl. 9, 1987, p 171-177
12. O.S. Es-Said, J.G. Morris, and R.J. De-Angelis, Effect of Extended Recovery on the Recrystallization Characteristics of Flash-Annealed Strip Cast 3004 Aluminum Alloy, *Mater. Charact.*, Vol 30, 1993, p 113-125
13. B. Noble, S.J. Harris, and K. Harlow, Mechanical Properties of Al-Li-Mg Alloys at Elevated Temperatures, *Proceedings of Aluminum-Lithium Alloys II*, TMS-AIME, 1984, p 65-77
14. I.G. Palmer, W.S. Miller, D.J. Lloyd, and M.J. Bull, Effect of Grain Structure and Texture on Mechanical Properties of Al-Li Base Alloys, *Proceedings of Aluminum-Lithium Alloys III*, Institute of Metals, 1985, p 565-575

15. C.W. Cho, B.A. Cheney, D.J. Lege, and J.I. Petit, Superplasticity of 2090 SPF Sheet at Hot Rolled Gauge, *J. Phys.*, Vol 48 (No. C3), Suppl. 9, 1987, p 277-283
16. J. Wadsworth, I.G. Palmer, D.D. Crooks, and R.E. Lewis, Superplastic Behavior of Aluminum-Lithium Alloys, *Proceedings of Aluminum-Lithium Alloys II*, TMS-AIME, 1984, p 111-135
17. H. Yoshida, S. Shirano, Y. Baba, T. Tsuzuku, and A. Takahashi, *J. Phys.*, Vol 48 (No. C3), Suppl. 9, 1987, p 269-275
18. E.A. Starke, Jr., T.H. Sanders, Jr., and I.G. Palmer, New Approaches to Alloy Development in the Al-Li System, *J. Met.*, Aug 1981, p 24-33